Renormalized transport of inertial particles in surface flows

Marco Martins Afonso[1,4]**, Andrea Mazzino**[2] **and Piero Olla**[3]

[1] Department of Mechanical Engineering, Johns Hopkins University, Baltimore, MD 21218, USA
[2] Department of Physics, University of Genova, and CNISM and INFN, Genova Section, via Dodecaneso 33, 16146 Genova, Italy
[3] ISAC-CNR and INFN, Cagliari Section, 09042 Monserrato (CA), Italy

E-mail: marcomar@fisica.unige.it and andrea.mazzino@unige.it

Abstract

Surface transport of inertial particles is investigated by means of the perturbative approach, introduced by Maxey (1987 *J. Fluid Mech.* **174** 441), which is valid when the deflections induced on the particle trajectories by the fluid flow can be considered small. We consider a class of compressible random velocity fields, mimicking the chaotic behaviour of nonlinearly interacting surface standing waves. The effect of recirculations is modelled by an oscillatory component in the Eulerian time-correlation profile. The main issue we address here is whether fluid velocity fluctuations, in particular the effect of recirculation, may produce nontrivial corrections to the streaming particle velocity. Our result is that a small (large) degree of recirculation is associated with a decrease (increase) of streaming with respect to a quiescent fluid. The presence of this effect is confirmed numerically, away from the perturbative limit. Our approach also allows us to calculate the explicit expression for the eddy diffusivity, and to compare both the efficiency of diffusive and ballistic transport and the different anisotropic character of dispersion induced by compressibility.

PACS numbers: 47.55.Kf, 47.55.D−, 47.27.−i

1. Introduction

Particle transport in laminar/turbulent flows is a problem of major importance in a variety of domains ranging from astrophysics to geophysics. For neutral (i.e., having the same density of the surrounding fluid) particles in incompressible flows the main quantity of interest is typically the rate at which the flow transports the scalar, e.g. a pollutant. For times that

---

[4] Present address: Institut de Mécanique des Fluides de Toulouse, Allée du Professeur Camille Soula, 31400 Toulouse, France.

are large compared to those characteristics of the flow field, transport is diffusive and is characterized by effective diffusivities (the so-called eddy diffusivities) which incorporate all the nontrivial effects played by the small-scale velocity on the asymptotic large-scale transport [1, 2]. Eddy diffusivities are expected on the basis of central limit arguments and can be calculated by means of asymptotic methods [3]. There are however situations where some, or all, of the hypotheses of the central-limit theorem break down with the result that in the asymptotic limit particles do not perform a Brownian motion and anomalous diffusion is observed [4, 5].

For compressible flows, large-scale transport is still controlled by eddy diffusivities but now transport rates are enhanced or depleted depending on the detailed structure of the velocity field [6].

For particles much heavier than the surrounding fluid, large-scale transport is still controlled by eddy diffusivities, which have been calculated in [7] exploiting asymptotic methods in the limit of small inertia.

Unlike what happens for neutral particles, an external force field can dramatically change transport properties. This is, for instance, the case when gravity is explicitly taken into account, with the result that a constant falling/ascending velocity sets in, thus dominating the particle long-time transport [8–16].

Our main aim here is to focus on transport of inertial particles in compressible media. Although our results are rather general (i.e., they apply to both one, two and three dimensions, and for a variety of external forces), the present study is physically motivated by the transport of floaters on a surface flow (e.g., the ocean surface) in the presence of strong surface winds. As we will see, the resulting dynamical equations for the particles moving on the (horizontal) surface under the action of strong (constant) winds are formally identical to those of heavy particles moving along the vertical under the action of gravity. A constant drift is thus expected, analogous to the settling velocity of a particle in suspension, in the presence of gravity. It is worth underlining that we only consider either of these two cases: surface transport of floaters on the horizontal, for which what happens in the lower layers of fluid is not relevant, *or* gravitational sedimentation of very heavy particles on the vertical, for which no added-mass effect arises. The former situation is more akin to that of foams or similar very light materials on the water surface, than to that of heavier sediments, whose dynamics is governed by the flow immediately underneath the water surface, as described e.g. in [17, 18]. We assert that both the surface drift, in the approximation considered, and the settling velocity of dense particles, can be described by the same formalism.

The specific problem we aim at investigating can be summarized as follows. The drift velocity v of a floater on a still water surface will be in general a complicated function of the wind velocity, U, and of other parameters like e.g. the floater structure and the surface roughness. A similar complication is expected in the way in which the drift velocity adapts to the wind and surface current variations. A rather minimal model could be obtained assuming a simple relaxation dynamics for the drift velocity:

$$\dot{v} = [\mathcal{V} - (v - u)]\gamma, \tag{1}$$

where u is the water surface velocity at the instantaneous location of the particle, $\gamma = \gamma(U - u, v - u)$ is the relaxation rate, and $\mathcal{V}$ is the terminal drift velocity (with $\mathcal{V} = \mathcal{V}(U - u)$). Since we expect $\mathcal{V}, u \ll U$, we may approximate $U - u \simeq U$ in the arguments of both $\mathcal{V}$ and γ, and, as a rough approximation, we may consider a linear relaxation dynamics: $\gamma(U, v - u) \simeq \gamma(U, 0)$. Under these hypotheses, (1) becomes formally identical to the equation for a small heavy particle in a viscous fluid, in the presence of a gravitational acceleration $\gamma \mathcal{V}$. In this case, γ^{-1} would be the Stokes time [19–22].

Now, spatio-temporal variations in the surface water velocity will lead to difficulties in the determination of a mean drift velocity. In other words, the mean drift may not necessarily be equal to what would be obtained by calculating a spatio-temporal average. In general, the interplay between currents and particle trajectories might lead to the result that either an enhanced or a reduced drift (with respect to the one in still fluid) might appear.

Here, we will assess the above possibility by means of an analytical (perturbative) approach in the same spirit of [10]. We will be able to identify an important dynamical feature of the carrying flow (the way through which it decorrelates in time) responsible for the different behaviour of the resulting drift with respect to the corresponding value in still fluid.

The paper is organized as follows. In section 2 the basic equations governing the time evolution of inertial particles in a prescribed flow are given, together with the perturbative expansion for strong sweeping or gravity. In section 3 we focus on compressible flows and compute the leading correction to terminal velocity. The same quantity is calculated in section 4 for incompressible Gaussian flows. In section 5 we analyse the phenomenon of particle diffusivity and, at the leading order, we study the diffusion coefficient; we also perform a quantitative comparison of the drift and diffusion displacements. Conclusions follow in section 6. The appendices are devoted (Appendix A) to displaying some additional analytical results, and (Appendix B) to provide some technical details of the calculation.

2. General equations

In the hypotheses of (1), the motion of a floater dragged by the wind, on a water surface with velocity field $\boldsymbol{u}(\boldsymbol{x}, t)$, will be described by

$$\begin{cases} \dot{\boldsymbol{x}}(t) = \boldsymbol{v}(t) \\ \dot{\boldsymbol{v}}(t) = \gamma[\boldsymbol{\mathcal{V}} + \boldsymbol{u}(\boldsymbol{x}(t), t) - \boldsymbol{v}(t)], \end{cases} \tag{2}$$

with the quantities $\boldsymbol{\mathcal{V}}$ and γ assumed as constants. We shall denote the direction of the vector $\boldsymbol{\mathcal{V}}$ as 'sweeping', and we align the axes such that it corresponds to the positive x_d component. To make contact with the dynamics of a heavy particle in a viscous fluid, we maintain d, that is the number of dimensions, arbitrary.

Given (Eulerian) characteristic length and time scales L and T and amplitude σ_u for the velocity field $\boldsymbol{u}$, we introduce the dimensionless Stokes, Kubo and Froude numbers S, K and F, defined as

$$S = \frac{1}{\gamma T}, \qquad K = \frac{\sigma_u T}{L} \qquad \text{and} \qquad F = \frac{\sigma_u}{\sqrt{\gamma \mathcal{V} L}}. \tag{3}$$

Note that such a definition of F is consistent with the 'identification' $\boldsymbol{g} = \gamma \boldsymbol{\mathcal{V}}$, if gravity is the 'sweeping' force under consideration (rather than wind). From now on, we adimensionalize times with γ^{-1} and velocities with σ_u, and denote the new adimensional variables with the same letters as before. In dimensionless form, the characteristic scales L and T of the velocity field, and the bare terminal velocity $\mathcal{V}$, will read

$$L = S^{-1}K^{-1}, \qquad T = S^{-1} \qquad \text{and} \qquad \mathcal{V} = SKF^{-2}. \tag{4}$$

The Kubo number K is basically the ratio of the life time and rotation time of a vortex, with $K \to 0$ corresponding to an uncorrelated regime, $K \to \infty$ to a frozen-like regime, and real turbulence being realized by $K = O(1)$.

We confine ourselves to situations where the particle trajectory, after some transient regime depending on the initial conditions, displays small deviations from the straight 'sweeping' line, thus allowing us to deal with a quasi-1D problem as a zeroth-order approximation [10]. This happens when the effect of streaming (or gravity) is much stronger than the deflections due

to the external flow. The particular case of vanishing inertia cannot thus be described by the following formalism.

We thus isolate in the solution $v = v(t)$ of (2) a term associated with the deviation from the behaviour in still fluid:

$$\tilde{v}(t) = \int_0^t dt' \, e^{t'-t} u(x^{(0)}(t') + \tilde{x}(t'), t'), \tag{5}$$

where

$$x^{(0)}(t) = x(0) + \mathcal{V}t + [v(0) - \mathcal{V}](1 - e^{-t}) \tag{6}$$

accounts for the unrenormalized sweep, and $d\tilde{x}/dt = \tilde{v}$, so that

$$\tilde{x}(t) = \int_0^t dt' \psi(t - t') u(x^{(0)}(t') + \tilde{x}(t'), t'), \qquad \psi(t) = 1 - e^{-t}. \tag{7}$$

A perturbative solution of (7) rests on the smallness of $\tilde{x}(t)$ in the argument of u. More precisely, it is necessary that $\tilde{x}(\tau_p) \ll L$, with τ_p being the correlation time for the fluid velocity $u(x(t), t)$ sampled by the particles. We can estimate

$$\tau_p \sim \min(T, L/\sigma_u, \mathcal{T}_{sw}), \qquad \mathcal{T}_{sw} \equiv L/\mathcal{V} = S^{-2}K^{-2}F^2, \tag{8}$$

with $\mathcal{T}_{sw}$ giving the contribution from sweep to decorrelation. In the absence of sweep effects, we know that $\tilde{x}(\tau_p)/L$ will be small provided either $K \ll 1$, or $K \gtrsim 1$ with $SK^{-2} \gg 1$ [23, 24]. In both regimes, indeed, the inertial particles will see u as a Kraichnan field [25, 26]. Sweeping acts to reduce the correlation time. A sufficient condition for small $\tilde{x}(\tau_p)/L$ turns out to be, in this case:

$$SKF^{-2} \gg 1, \tag{9}$$

that is the strong-sweep condition $\mathcal{V} \gg \sigma_u$ (no condition is put on γ). Note that, for sufficiently large S, this condition and the one for a Kraichnan regime $K \ll 1$ overlap. We assume u as a homogeneous, isotropic, stationary, zero-mean random flow and we denote by $\langle \cdot \rangle$ the ensemble average over its realizations.[5] From a physical point of view, this smooth random (in general compressible) flow can be used to model the chaotic spatio-temporal behaviour arising when high-amplitude surface standing waves interact nonlinearly [27, 28].

We are interested in finding the steady-state average particle velocity, which corresponds, in (5), to averaging over u and taking $t \to +\infty$. Taylor expanding in $\tilde{x}$ the right-hand side (RHS) of (5), and using (7) recursively, allows us to calculate the correction to sweep. We clearly obtain $\langle \tilde{v}^{(1)}(t) \rangle = 0$. Then, we have

$$\left\langle \tilde{v}_i^{(2)}(t) \right\rangle = \int_0^t dt' \psi(t - t') \langle \mathcal{U}_j(t') \partial_j \mathcal{U}_i(t) \rangle, \tag{10}$$

where

$$\mathcal{U}(t) = u(x^{(0)}(t), t) \tag{11}$$

(i.e., the unperturbed flow is 'sampled' on the *fixed* 'sweeping' line). As it is well known, the lowest order correction to $\mathcal{V}$ vanishes if u is incompressible. In this case, in order to obtain non-zero corrections to the falling velocity, it is necessary to go to higher orders in the perturbative expansion of (5)–(7) [10]. Namely, in the incompressible case, we have

$$\left\langle \tilde{v}_i^{(3)}(t) \right\rangle = \int_0^t dt' \psi(t - t') \int_0^{t'} dt'' [\psi(t' - t'') - \psi(t - t'')] \langle \mathcal{U}_k'' \mathcal{U}_j' \partial_j \partial_k \mathcal{U}_i \rangle. \tag{12}$$

---

[5] For the problem of surface transport, note that, in general, the wind will also cause a mean drift of the fluid (Stokes drift) $\langle u \rangle$, in the same direction of U, but with a much smaller modulus (also with respect to $\mathcal{V}$). Our approach is thus valid when passing to the frame of reference moving with $\langle u \rangle$, and considering an 'effective', reduced wind velocity $U \mapsto U - \langle u \rangle$.

The latter quantity is zero if $\boldsymbol{u}$ is a Gaussian field. Thus, for incompressible Gaussian flows, one has to compute the next order:

$$
\left\langle \tilde{v}_i^{(4)}(t) \right\rangle = \int_0^t \mathrm{d}t' \int_0^{t'} \mathrm{d}t''\, \psi(t-t')\psi(t'-t'')
$$
$$
\times \left[\int_0^t \mathrm{d}t'''\, \psi(t-t''') - \int_0^{t''} \mathrm{d}t'''\, \psi(t''-t''') \right] \partial_j \partial_l \langle \mathcal{U}_i \mathcal{U}_k'' \rangle \partial_k' \langle \mathcal{U}_j' \mathcal{U}_l''' \rangle. \tag{13}
$$

In section 3 we provide an example of compressible flow, for which (10) applies. Due to the difficulty of dealing analytically with non-Gaussian flows, we will not provide applications of (12). In contrast, in section 4, we will focus on an incompressible Gaussian flow, for which (13) is the leading correction to the falling velocity.

3. Compressible flows

Let us focus on the compressible case and compute the average in (10). Clearly we only need to compute the component with index $i = d$ (in our convention it is assumed positive if pointing along the mean flow).

Let us first analyse $d > 1$. Introducing the well-known compressibility degree, $\mathcal{P} \equiv \langle (\partial_j u_j)^2 \rangle / \langle (\partial_k u_l)(\partial_k u_l) \rangle \in [0,1]$,[6] the expression for the Eulerian pair correlation tensor $R_{ij}(\boldsymbol{x},t) \equiv \langle u_i(\boldsymbol{x},t) u_j(\boldsymbol{0},0) \rangle$ can be deduced from the Helmholtz decomposition

$$
R_{ij}(\boldsymbol{x},t) = [(1-d\mathcal{P})\partial_i\partial_j - (1-\mathcal{P})\delta_{ij}\partial^2]\mathcal{R}(x,t) \tag{14}
$$

by imposing the form of the scalar $\mathcal{R}(x,t)$. Let us assume a Gaussian behaviour both in space and in time, with temporal oscillations described by ω (adimensionalized with γ for the sake of consistency):

$$
\mathcal{R}(x,t) = \frac{1}{d(d-1)S^2K^2} \cos(\omega t)\, \mathrm{e}^{-S^2t^2/2}\, \mathrm{e}^{-S^2K^2x^2/2}. \tag{15}
$$

Substituting into (14), we obtain

$$
R_{ij}(\boldsymbol{x},t) = \frac{1}{d(d-1)} \cos(\omega t)\mathrm{e}^{-S^2t^2/2}\mathrm{e}^{-S^2K^2x^2/2}
$$
$$
\times\{(1-d\mathcal{P})S^2K^2 x_i x_j + \delta_{ij}[(d-1) - (1-\mathcal{P})S^2K^2x^2]\} \tag{16}
$$

and thus

$$
\partial_j R_{ij}(\boldsymbol{x},t) = \frac{\mathcal{P}S^2K^2}{d} \cos(\omega t)\, \mathrm{e}^{-S^2t^2/2}\, \mathrm{e}^{-S^2K^2x^2/2}[S^2K^2x^2 - (d+2)]x_i. \tag{17}
$$

The case $d = 1$ automatically implies $\mathcal{P} = 1$, and expressions (14)–(16) are ill-posed. However, if one neglects them and considers expression (17) directly, everything is consistent and also the 1D case can be investigated by means of the same formalism. Our choice of obtaining the latter equation passing through the former three for $d > 1$ is simply dictated by the simple and important meaning that the compressibility degree plays: the lower bound $\mathcal{P} = 0$ denotes incompressible flows and the upper bound $\mathcal{P} = 1$ perfectly compressible (potential) ones.

It is interesting to study under what conditions the tensor (16) is positive definite (for $d > 1$). One can note that, as in our calculations it always appears under some integral, it is sufficient to study the separations $x < L$, because the Gaussian factor makes the contribution from larger distances negligible. Thus, using (4), $S^2K^2x^2|_{x<L} < 1$, and therefore the quantity

---

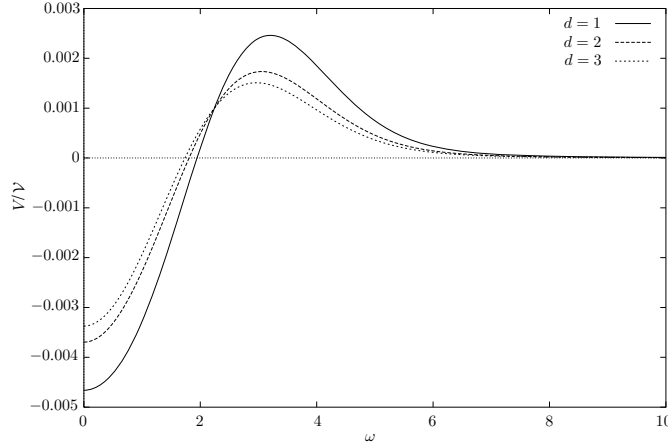[6] by virtue of homogeneity, this factor turns out to be space independent.

Figure 1. Leading-order correction to the terminal velocity, normalized with the corresponding bare value, as a function of ω, for $d = 1, 2$ and 3. Here, $\mathcal{P} = 1 = S$ and $F = 0.1 = K$.

in square braces beside δ_{ij} is always positive in this case. Then, the investigation of the tensorial part suggests that R_{ij} would surely be positive definite (for the only relevant interval, $x < L$) when $\mathcal{P} < d^{-1}$, if the time-oscillating factor were absent. This tells us that, at low compressibility, the introduction of the temporal oscillations corresponds to the appearance of negatively correlated areas, and tuning the parameter ω one can change the relevance of the recirculating flow. Under our assumptions, performing the simple change of variables $\tau \equiv t - t'$, at very large times $\forall d$ expression (10) for the 'sweeping' component simplifies to

$$V \equiv \lim_{t \to \infty} \left\langle \tilde{v}_d^{(2)}(t) \right\rangle = \frac{\mathcal{P} S^3 K^3}{d F^2} \int_0^\infty d\tau \, \tau \left[\frac{S^4 K^4}{F^4} \tau^2 - (d+2) \right] \cos(\omega\tau) \psi(\tau) \, e^{-\Gamma^2 \tau^2 / 2}, \qquad (18)$$

where

$$\Gamma = S\sqrt{1 + \Delta^2} \approx \tau_p^{-1} \qquad \text{and} \qquad \Delta = SK^2 F^{-2} \qquad (19)$$

are respectively the decorrelation rate, and the ratio $T/\mathcal{T}_{sw}$. The last integral in (18) can be carried out analytically and the result can be expressed in terms of error functions, but for the sake of simplicity it is not reported here (see (A.1) in Appendix A). Out of the six parameters in play, we note that V is exactly linear in $\mathcal{P}$, and coherently vanishes in the incompressible case, thus we can fix $\mathcal{P} = 1$ for the rest of this section without loss of generality. Let us then analyse the dependence of V on the five remaining parameters (ω, S, K, F and d).

- A simple look at the structure of the integrand in (18), or at the final expression (A.1), suggests that $V \to 0$ for $\omega \to \infty$. Equation (A.2) displays the simplification occurring in the static case $\omega = 0$. In figures 1 and 2, we plot the ratio $V/\mathcal{V}$ between the leading correction to the terminal velocity and its bare value, as a function of the frequency. We note that small values of the frequency are associated with a negative renormalization, while high-frequency flows are characterized by an increased terminal velocity. A similar situation can be shown to arise as a result of finite-T corrections, in the transport of inertial particles by a Kraichnan velocity field [24]. We can thus conclude that (at least for $\mathcal{P} < d^{-1}$), if the extension of negative regions in the time-correlation profile is sufficiently small (large), the renormalized streaming is smaller (larger) than the bare
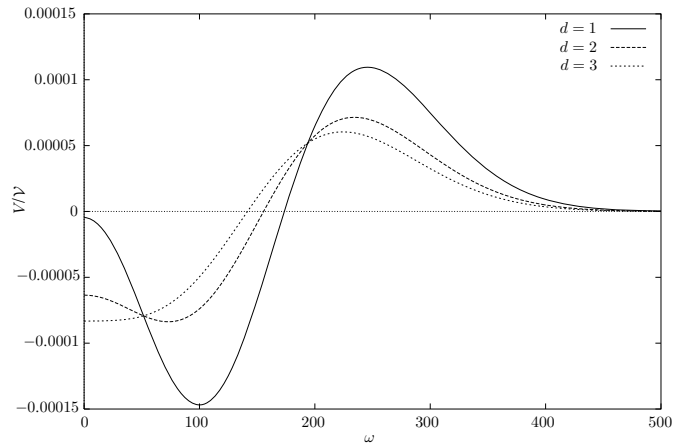
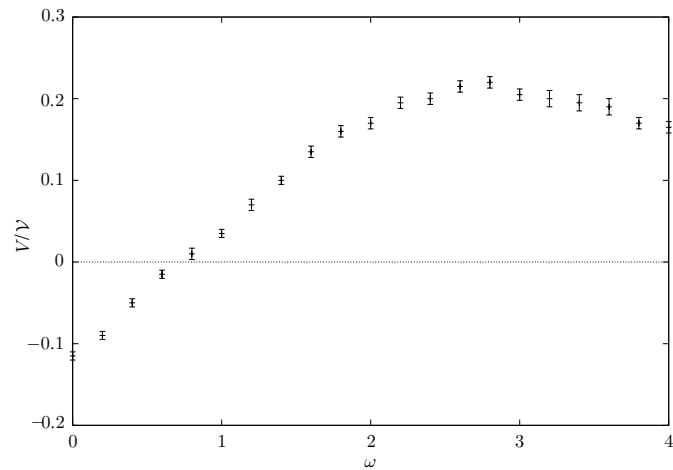**Figure 2.** Same as in figure 1 but with $S = 10$ and $F = 1 = K$.

Figure 3. Leading-order correction to the terminal velocity versus ω, from a numerical simulation of transport by a 2D fully compressible velocity field. Parameters of the simulation: $S = 2$, $K = 0.5 = F$.

one, which amounts to saying that the absence (presence) of areas of recirculation helps to make the particles travel slower (faster) than in the case of still fluid. As we can see from figure 3, this conclusion is confirmed also for finite values of the expansion parameter; in the case in exam: $SKF^{-2} = 4$. To this goal, a numerical simulation of transport by a synthetic velocity field has been carried on, in which the velocity was generated from a superposition of random Fourier modes with Gaussian spectrum, with a 4-point interpolation between grid points to integrate the particle trajectories. Instead of an oscillating Gaussian profile (15) for the time correlation, an oscillating exponential has been adopted, which is easily obtained imposing a Langevin dynamics on the Fourier modes. In all simulations, 64^2 Fourier modes have been utilized for a domain size of 10 times the correlation length of the flow, this is sufficient to avoid periodicity problems
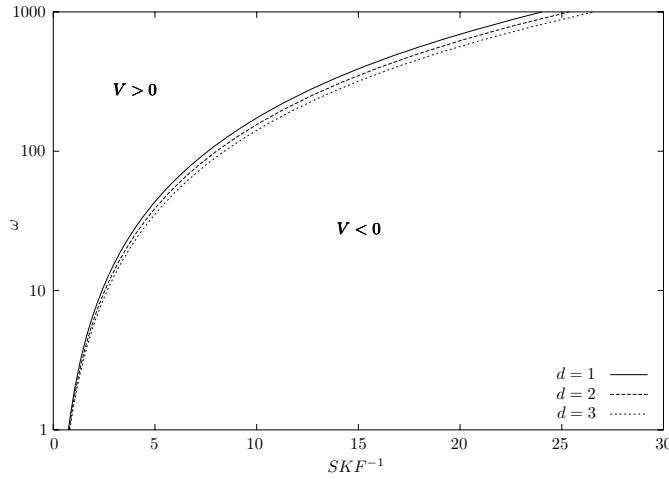
Figure 4. Separatrix between regions of increased (upper left) and decreased (lower right) sweeping in the plane ω versus SKF^{-1}, for $d = 1$, 2 and 3 (solid, dashed and dotted lines, respectively). The plot namely corresponds to fixed values of $K = 1$ and $F = 0.1$, but by varying these parameters only negligible changes appear (unless $K \ll 1$).

with falling particles sampling many times the same eddy before this decays. To obtain good statistics, runs of 100 correlation times with 2×10^4 particles have been sufficient.

- For $T \gg \mathcal{T}_{sw}$ (see (8)) the integrand in (18) will depend solely on $\mathcal{T}_{sw}$. Thus, if one studies the zero of expression (18) (i.e., the boundary that separates accelerating and decelerating situations, at the lowest order), the most interesting plot is represented by the separatrix line in the plane ω versus SKF^{-1} for not-too-small values of K, such that S, K and F appear only via this combination. In figure 4, the lower right area corresponds to deceleration and the upper left to acceleration in sweeping. Note that low (respectively, high) values of SKF^{-1} correspond preferentially to situations of increased (respectively, decreased) terminal velocity.

- The same simplification into a dependence on SKF^{-1} only is not valid for the whole expression (18) itself, because of the prefactor. Nevertheless, an interesting rescaling property can be shown to hold when the parameters belong to a specific range. First of all, if one considers the ratio $V/\mathcal{V}$, the prefactor $S^3 K^3 F^{-2}$ in (18) becomes $S^2 K^2$, i.e. $(SKF^{-1})^2 F^2$. Now, suppose that $T \gg \mathcal{T}_{sw}$, such that, in the exponent of the Gaussian factor, $\Delta \gg 1$ and thus $\Gamma \simeq (SKF^{-1})^2$. Also, suppose that $SKF^{-1} \gg 1$, so that the same Gaussian is very narrow. This allows us to Taylor expand $\psi(\tau) \sim \tau$. Then, starting from a situation in which such approximations hold (e.g., the case plotted in figure 2), suppose to rescale SKF^{-1} by a factor α. The expression in square brackets and the simplified Gaussian factor remain unchanged upon rescaling τ by α^{-2}, and consequently the cosine does not change if ω is rescaled by α^2. Keeping into account the τ factor explicitly appearing in (18), the one coming from the Taylor expansion of $\psi(\tau)$ and the integration variable differential, one deduces that the integral gets rescaled by $(\alpha^{-2})^3 = \alpha^{-6}$. By considering also the above-mentioned prefactor $(SKF^{-1})^2 F^2$, one can argue that, under these approximations: (I) upon rescaling SKF^{-1} by α while keeping F fixed, figure 2 simply reproduces itself by rescaling ω by α^2 on the abscissae and $V/\mathcal{V}$ by α^{-4} on the ordinates; (II) upon rescaling F by β while keeping SKF^{-1} fixed, figure 2 simply expands vertically by β^2 without changing horizontally.
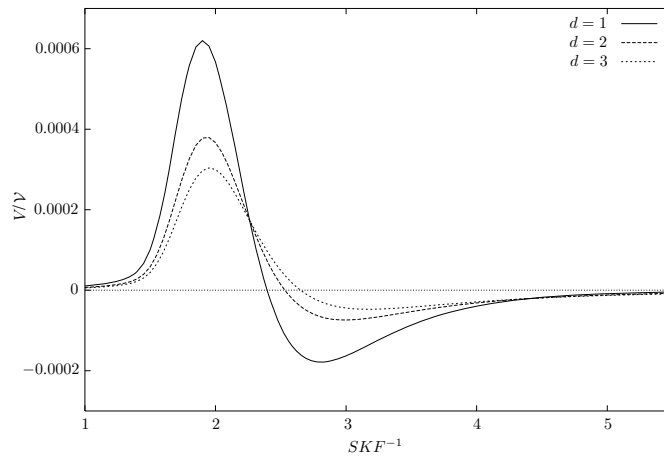
Figure 5. Leading-order correction to the terminal velocity, normalized with the corresponding bare value, as a function of SKF^{-1}, for $d = 1, 2$ and 3. Here, $\mathcal{P} = 1$ and $\omega = 10$. The plot namely corresponds to fixed values of $K = 0.1 = F$, and by varying these parameters it gets rescaled as explained in the text.
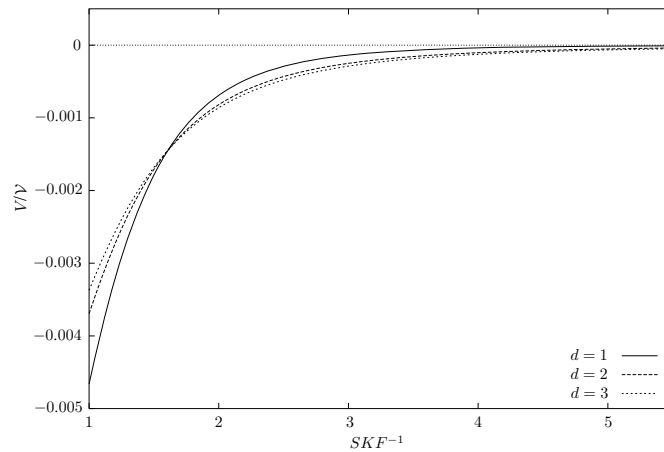

Figure 6. Same as in figure 5 but for the static case $\omega = 0$.

In figures 5 and 6, $V/\mathcal{V}$ is now plotted as a function of SKF^{-1} for different values of the frequency.

- The dependence on the dimension seems to be very weak. In particular, all our plots show little difference between $d = 1, 2$ and 3, with the one-dimensional case showing the largest peaks. Moreover, figures 1–2 and 5–6 are peculiar in the sense that the three lines always cross in the very same points. We have not been able yet to identify the underlying analytical mechanism causing this phenomenon, which however seems to be very robust because it is also confirmed by plotting e.g. a fictitious four-dimensional case.

4. Incompressible Gaussian flows

The role of ω, i.e. of oscillations in the velocity correlation profile, in determining the sign of the terminal velocity renormalization, is completely different in the case of a Gaussian incompressible flow. As discussed in [10], this requires going to fourth order in the perturbation expansion (see (13)).

The interest of the problem is rather formal, as non-Gaussianity in realistic turbulent flows is likely to play an important role. Nevertheless, simple analytical expressions can be obtained in the small-sweep regime, with rapid decorrelation imposed through smallness of T. More precisely, we assume

$$SK^2 F^{-2} \ll 1, \qquad S \gg \max(1, K^2). \tag{20}$$

In this limit, the decorrelation Γ is dominated by the Eulerian correlation time $T \ll \tau_S = 1$ and the total displacement in a time T will be much smaller than the characteristic scale $L = S^{-1} K^{-1}$.

As detailed in Appendix B, this allows one to expand the integrand in (13) in both space (the correlations $\langle \mathcal{U}\mathcal{U} \rangle$) and time (the propagator ψ). Note that, in these approximations, the precise form of the spatial correlation (B.1) has no influence on the sign of the correction, as only its second derivative computed at merged points, (B.3), enters the calculation. A simpler expression for the settling velocity renormalization, illustrating the changing sign behaviour, is obtained with a temporal correlation in the form:

$$h(t) = \mathrm{e}^{-S|t|} \cos(\omega t). \tag{21}$$

Substituting into (B.7), we obtain

$$\hat{V} \equiv \lim_{t \to \infty} \left\langle \tilde{v}_d^{(4)}(t) \right\rangle = \frac{(d+1)(d+2)\hat{f}^2 K^5}{4(d-1)S^2 F^2} Q\left(\frac{\omega}{S}\right), \tag{22}$$

where

$$Q(a) = \frac{11 - 94a^2 + 177a^4 - 45a^6 - 7a^8 - a^{10}}{(1+a^2)^7}.$$

Using (4), we see that $\hat{V}/\mathcal{V} \propto S^{-3} K^4$, corresponding to an $O(S^{-3} K^4)$ renormalization of γ, to be compared with the $O(S^{-1} K^2)$ renormalization observed in the fully compressible 1D case [24]. The plot of the function $Q(a)$ is shown in figure 7. It was observed in [10], in the case of strong sweep, and in the absence of oscillations for $h(t)$, that the correction to the settling velocity is positive. We see in figure 7 that the same situation occurs in the small sweep regime, while we can also identify a range of values of ω for which the falling velocity is decreased. However, the renormalization effect quickly becomes negligible at large ω. In any case, we were able to show that, at least in some particular instances, the presence or absence of compressibility makes the role of ω the opposite passing from one case to the other.

5. Particle diffusivity

After computing the terminal velocity, it is interesting to study how the particle diffuses. In particular, we would like to find the diffusion coefficient

$$D = \lim_{t \to \infty} \frac{\langle [\boldsymbol{x}(t) - \langle \boldsymbol{x} \rangle(t)]^2 \rangle}{2dt}, \tag{23}$$
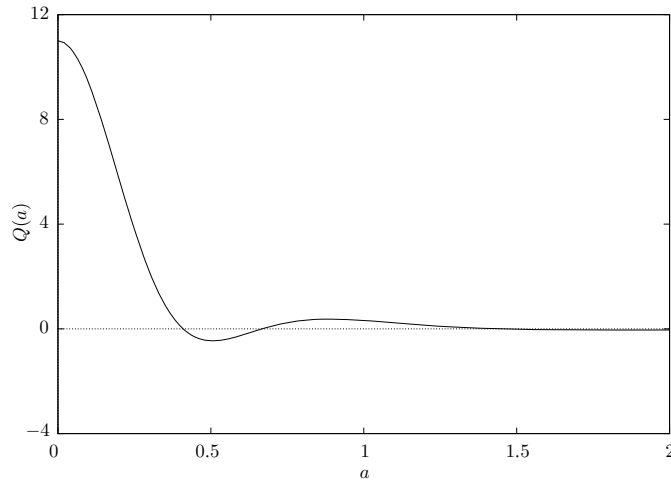
to be compared with the diffusivity of a fluid parcel,

10

Figure 7. The profile of the function Q.

$$\mathcal{D} \sim \sigma_u^2 T = S^{-1}.$$

With this aim, we firstly note that the term $\boldsymbol{x}^{(0)}$ in (6) does not contribute to expression (23), because it is independent of the external random flow. It is thus sufficient to investigate $\tilde{\boldsymbol{x}}$ from (7), and namely (using (11)) its leading order

$$\tilde{\boldsymbol{x}}^{(1)}(t) = \int_0^t \mathrm{d}t' \psi(t - t')\boldsymbol{\mathcal{U}}(t').$$

For zero-mean flows we have $\langle \tilde{\boldsymbol{x}}^{(1)}(t) \rangle = 0$, therefore

$$D^{(1)} = \lim_{t \to \infty} \frac{1}{2dt} \int_0^t \mathrm{d}t' \psi(t - t') \int_0^t \mathrm{d}t'' \, \psi(t - t'') \langle \mathcal{U}_i(t')\mathcal{U}_i(t'') \rangle. \tag{24}$$

Looking at (24), we see that $\psi(t - t')$ and $\psi(t - t'')$ differ from 1 only for t' and t'' close to t, and for $t \to \infty$ we can disregard this contribution. Thus, $D^{(1)}$ is simply the diffusivity of a random walker with velocity $\boldsymbol{\mathcal{U}}$, and we have the standard expression

$$D^{(1)} = \frac{1}{d} \int_0^\infty \mathrm{d}t \, \langle \mathcal{U}_i(0)\mathcal{U}_i(t) \rangle. \tag{25}$$

If we now restore our space-and-time Gaussian oscillating correlation, we can replace the average in (25) with the trace of expression (16), computed at space-time separation $(\boldsymbol{\mathcal{V}}t, t)$, and we obtain the result:

$$D^{(1)} = \frac{\sqrt{\pi}S^4}{\sqrt{2}d^2\Gamma^5} \mathrm{e}^{-\omega^2/2\Gamma^2} \left\{ (d - 1)\Delta^4 + \left[(2d - 1) + \left(\frac{\omega}{S} \right)^2 \right] \Delta^2 + d \right\}, \tag{26}$$

with Γ and Δ given in (19).

Note that the compressibility degree $\mathcal{P}$ disappears in the trace R_{ii}, and thus does not affect the diffusion coefficient. It can easily be seen from (26) that $D^{(1)}$ depends on S and SKF^{-1} only, and not on K and F separately. Figures 8 and 9 show the behaviour of the diffusivity as a function of the frequency. In figures 10 and 11, the diffusivity is plotted versus SKF^{-1}. In all cases, plotted is the ratio of the particle-to-fluid diffusivities, $D^{(1)}/\mathcal{D}$. As a further step, one can also investigate the different diffusive behaviour between the 'sweeping' direction and each of the orthogonal ones (if any). In particular, one obtains
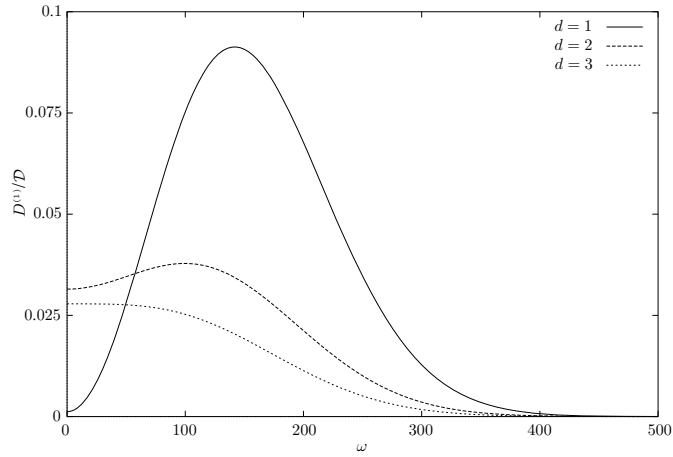
11

Figure 8. Leading-order expression for the total diffusivity, divided by the corresponding fluid-particle value, as a function of ω, for $d = 1, 2$ and 3. Here, $S = 10$, $\forall K = F$ and $\forall \mathcal{P}$.
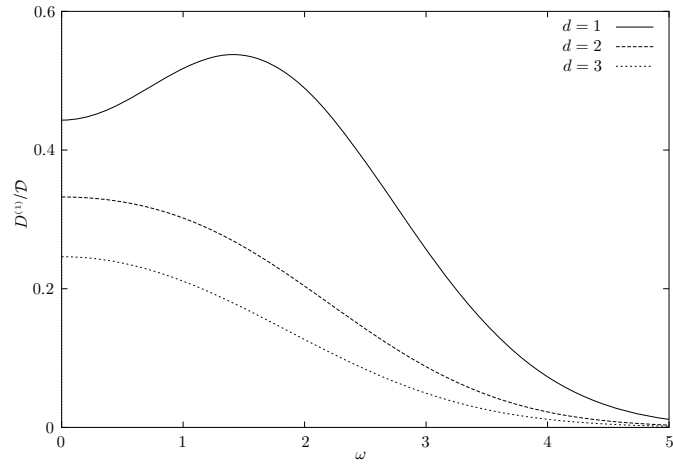

Figure 9. Same as in figure 8 but with $S = 1$.

$$D_{\parallel}^{(1)} \equiv \lim_{t \to \infty} \frac{\left\langle \left[\tilde{x}_d^{(1)}(t) \right]^2 \right\rangle}{2dt} = \frac{\sqrt{\pi} S^4}{\sqrt{2} d^2 \Gamma^5} \, \mathrm{e}^{-\omega^2/2\Gamma^2}$$

$$\times \left\{ (1 - \mathcal{P}) \Delta^4 + \left[(2 - \mathcal{P}) + \mathcal{P} \left(\frac{\omega}{S} \right)^2 \right] \Delta^2 + 1 \right\} \tag{27}$$

and

$$D_{\perp}^{(1)} \equiv \frac{D^{(1)} - D_{\parallel}^{(1)}}{d - 1} = \frac{\sqrt{\pi} S^4}{\sqrt{2} d^2 \Gamma^5} \mathrm{e}^{-\omega^2/2\Gamma^2}$$

$$\times \left\{ \frac{d + \mathcal{P} - 2}{d - 1} \Delta^4 + \left[\frac{2d + \mathcal{P} - 3}{d - 1} + \frac{1 - \mathcal{P}}{d - 1} \left(\frac{\omega}{S} \right)^2 \right] \Delta^2 + 1 \right\} \tag{28}$$

(note that $D^{(1)} = D_{\parallel}^{(1)}$ for $d = 1$ because there $\mathcal{P} = 1$).
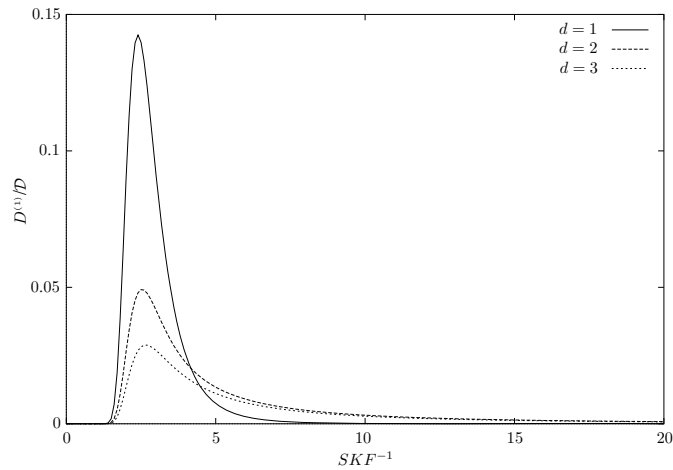
Figure 10. Leading-order expression for the total diffusivity, divided by the corresponding fluid-particle value, as a function of SKF^{-1}, for $d = 1, 2$ and 3. Here, $\omega = 10$ and $S = 1, \forall \mathcal{P}$.
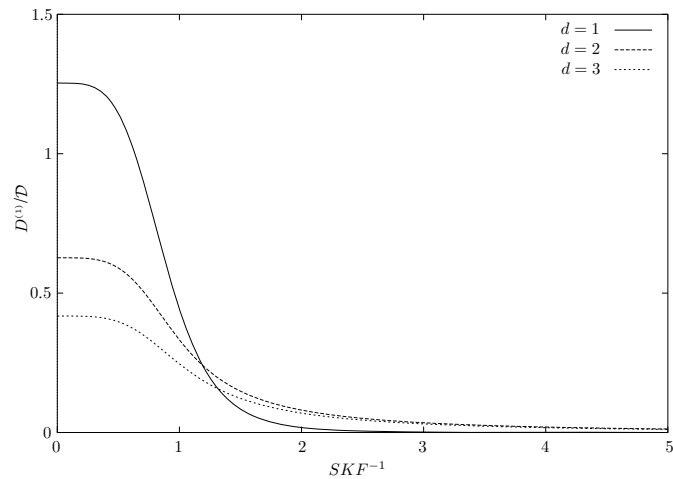

Figure 11. Same as in figure 10 but for the static case $\omega = 0$.

It is worth noting that the compressibility degree now appears again in the two previous expressions: only the total diffusivity is independent of it. Expressions (27) and (28) easily allow us to investigate the effect of compressibility on the type of anisotropy in the dispersion process. To be more specific, we note that, for both the $d = 2$ and $d = 3$ cases, the assumption $\omega/S \ll 1$ leads to the conclusion $D_{\perp}^{(1)} < D_{\parallel}^{(1)}$ for the incompressible case ($\mathcal{P} = 0$), while the opposite $\left(D_{\perp}^{(1)} > D_{\parallel}^{(1)}\right)$ holds for the potential case $\mathcal{P} = 1$.

5.1. Comparison between drift and diffusion displacements

It is now possible to compare the contributions to a particle displacement given by drift and by diffusion. At the time t large enough to forget about initial conditions, the typical
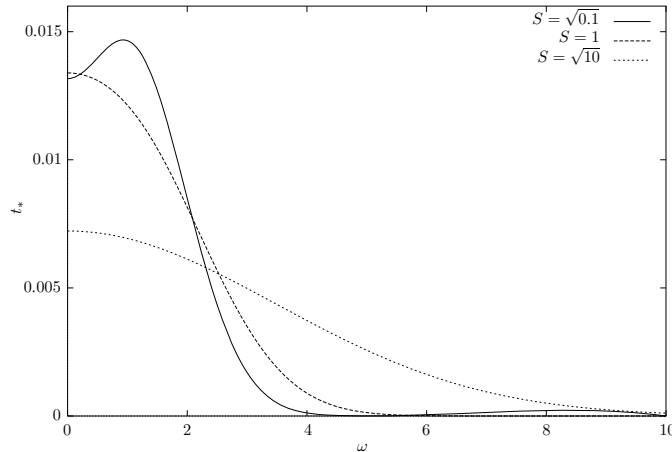
Figure 12. Crossover time, as a function of ω, between diffusion- and drift-dominated particle displacement. Here, $d = 2$, $\mathcal{P} = 1$, $F = 0.1$ and $SKF^{-1} = 1$.

displacement due to drift is about $(\mathcal{V} + V)t$, while the diffusive one is of the order of $\sqrt{2dD^{(1)}t}$. The former clearly dominates at large times, while the latter represents the leading value of the displacement at short times. We can thus define the crossover time

$$t_* \equiv \frac{2dD^{(1)}}{(\mathcal{V} + V)^2},$$

after which drift represents the dominant mechanism and diffusion can be neglected.

　　Focusing on the two-dimensional potential-flow case, in figure 12 such crossover time (remember that, in our convention, it is adimensionalized with γ) is plotted as a function of the frequency for three different values of the Stokes number. Note, the peak that can occur in t_* at a critical value of ω when the other parameters assume certain values.

6. Conclusions and perspectives

We investigated the drift and diffusion behaviour of inertial particles in random flows, in the limit in which the expansion 'à la Maxey' works, i.e. in the presence of strong sweeping, or of an underlying flow varying rapidly, such that the resulting motion at the scales of interest is almost rectilinear. This picture can be applied both to the settling of heavy particles due to gravity, and, more interestingly, to the motion of floaters, e.g. on a water surface, under the action of a streaming wind. Imposing an oscillating Gaussian form to the external flow, we found the analytical expressions of the renormalized terminal velocity and of the effective diffusivity, as functions of the oscillation frequency and of the Stokes, Kubo and Froude numbers. The latter three quantities often appear not independently from one another, but rather as an overall combination. For the terminal velocity, we found that, if the flow is compressible, small values of the frequency are associated with a negative renormalization with respect to the corresponding value in still fluids, while high-frequency flows are characterized by an increased asymptotic speed. In some cases, the opposite behaviour holds as a function of the parameter SKF^{-1}, or as a function of ω itself if the flow is Gaussian and incompressible. The effective diffusivity can show some 'resonant' peaks as a function both of ω and of SKF^{-1}. The role played by the compressibility degree $\mathcal{P}$ is apparently quite simple: it appears linearly in the leading correction to the renormalized terminal velocity (so that, for incompressible

flows, higher-order effects have to be considered), and it does not influence the total effective diffusivity, because the dependence on $\mathcal{P}$ shown by the components of the diffusivity parallel and orthogonal to the sweeping direction is such as to create an overall compensation. However, we were able to show that the value of $\mathcal{P}$ can have relevant consequences on the role played by ω on the renormalized streaming. In particular, we can conclude that for compressible flows (at least when the compressibility degree is not too high, but neither too low in order to have non-negligible effects), the introduction of time oscillations in the velocity correlation function mimics the presence of areas of recirculation, or in other words of negatively correlated regions in the flow, and is associated with an increase in the particle terminal velocity; in contrast, a decrease is found for slow or no oscillations (for which the Eulerian time correlation is positive). In all cases, we also found that the dependence on the dimension ($d = 1, 2, 3$) is quite weak.

Acknowledgment

Appendix A. Exact results for the compressible case

The result of the integral in (18), computed with MATHEMATICA (which makes use of complex variables), is

$$
V = \frac{\mathcal{P} S^5 K^3}{dF^2 \Gamma^7} \left\{ -\sqrt{\frac{\pi}{2}} S^2 \Re \left[\left((d-1)\Delta^4 + \left((2d+1) + \left(\frac{\omega+\mathrm{i}}{S} \right)^2 \right) \Delta^2 + (d+2) \right) \right. \right.
$$
$$
\left. \times (1 - \mathrm{i}\omega)\mathrm{e}^{(1-\mathrm{i}\omega)^2/2\Gamma^2} \left(1 - \mathrm{erf}\left(\frac{1-\mathrm{i}\omega}{\sqrt{2}\Gamma} \right) \right) \right] - \Gamma\Delta^2 + \sqrt{\frac{\pi}{2}} S^2 \omega \mathrm{e}^{-\omega^2/2\Gamma^2}
$$
$$
\left. \times \left[(d-1)\Delta^4 + \left((2d+1) + \left(\frac{\omega}{S} \right)^2 \right) \Delta^2 + (d+2) \right] \left| \mathrm{erf}\left(\frac{\mathrm{i}\omega}{\sqrt{2}\Gamma} \right) \right| \right\}, \quad \text{(A.1)}
$$

where erf is the usual error function, $\Re$ denotes the real part, and Γ, Δ were defined in (19).

In the static case ($\omega = 0$), this expression simplifies to

$$
V|_{\omega=0} = -\frac{\mathcal{P} S^5 K^3}{dF^2 \Gamma^7} \left\{ \Gamma\Delta^2 + \sqrt{\frac{\pi}{2}} S^2 \, \mathrm{e}^{1/2\Gamma^2} \left[1 - \mathrm{erf}\left(\frac{1}{\sqrt{2}\Gamma} \right) \right] \right.
$$
$$
\left. \times \left[(d-1)\Delta^4 + \left((2d+1) - \frac{1}{S^2} \right) \Delta^2 + (d+2) \right] \right\}. \quad \text{(A.2)}
$$

Appendix B. Technical details for the incompressible case

Setting $\mathcal{P} = 0$, we can rephrase (14) following [10] and write

$$
R_{ij}(\boldsymbol{x}, t) = \left\{ g(x)\delta_{ij} + [f(x) - g(x)]\frac{x_i x_j}{x^2} \right\} h(t), \quad \text{(B.1)}
$$

where $f(x)$ and $g(x)$ are such as to ensure incompressibility, and we assume $h(0) = 1$. In this way, the integrand of (13), with $i = d$, can be rewritten as

$$
H(t''', t', t'', t) \equiv \partial_j \partial_l \langle \mathcal{U}_d \mathcal{U}_k'' \rangle \partial_k' \langle \mathcal{U}_j' \mathcal{U}_l''' \rangle
$$
$$
= \mathrm{sgn}(t' - t''')h(t - t'')h(t' - t''') \left[\frac{d+1}{r} f'(r)g'(s) + \frac{d+1}{d-1} f''(r)f'(s) \right], \quad \text{(B.2)}
$$

15

with $s = \mathcal{V}|t' - t'''|$ and $r = \mathcal{V}|t - t''|$ (primes on f and g now indicate differentiation with respect to the corresponding variables). Note that H is invariant under changes of third and fourth variables, while it flips its sign when changing first and second variables; homogeneity also implies that $H(t''', t', t'', t)$ is a function of $t - t''$ and $t' - t'''$ only.

The first condition assumed in (20), corresponding to a quasi-uniform field, allows us to expand the functions f and g in (B.1) in powers of the spatial variable:

$$R_{ij}(\boldsymbol{x}, t) \simeq \left[\frac{1}{d} + \frac{1}{2}g''(0)x^2\right]\delta_{ij} + \frac{1}{2}[f''(0) - g''(0)]x_i x_j$$

(here, $f'(0) = 0 = g'(0)$ to ensure smoothness, and $f(0) = g(0) = d^{-1}$ by construction). The incompressibility constraint gives us $g''(0) = [(d + 1)/(d - 1)]f''(0)$. Recalling the meaning of L and our adimensionalization of lengths in (4), we can introduce

$$\hat{f} \equiv L^2 f''(0) \iff f''(0) = S^2 K^2 \hat{f}, \tag{B.3}$$

where $\hat{f}$ is now $O(1)$.

Looking at (B.2), we see that we must expand the first-order derivatives; this gives us

$$H(t''', t', t'', t) = (t' - t''')\mathcal{V}h(t - t'')h(t' - t''')\left[(d + 1)f''(0)g''(0) + \frac{d + 1}{d - 1}f''(0)^2\right]$$

$$= \frac{(d + 1)(d + 2)S^5 K^5 \hat{f}^2}{(d - 1)F^2}h(t - t'')h(t' - t''')(t' - t'''). \tag{B.4}$$

We then see that the contribution from the space correlation always has the same sign.

The integrals in (13) can be written in the equivalent form:

$$\left\langle \tilde{v}_i^{(4)}(t) \right\rangle = \int_0^t d\tau\, \psi(\tau) \left\{ \int_{-\tau}^{t-\tau} d\tau' \int_{\tau+\tau'}^t d\tau''\, \psi(\tau + \tau')\psi(\tau'' - \tau - \tau') \right.$$

$$\left. + \int_\tau^t d\tau'' \int_{\tau''-\tau}^{t-\tau} d\tau'\, \psi(\tau'' - \tau)\psi(\tau + \tau' - \tau'') \right\} H(\tau', 0, 0, \tau''),$$

leading to the expression for $\hat{V} \equiv \lim_{t\to\infty}\left\langle \tilde{v}_d^{(4)}(t) \right\rangle$:

$$\hat{V} = \int_0^\infty d\tau\, \psi(\tau) \left\{ \int_{-\tau}^\infty d\tau' \int_{\tau+\tau'}^\infty d\tau''\, \psi(\tau + \tau')\psi(\tau'' - \tau - \tau') \right.$$

$$\left. + \int_\tau^\infty d\tau'' \int_{\tau''-\tau}^\infty d\tau'\, \psi(\tau'' - \tau)\psi(\tau + \tau' - \tau'') \right\} H(\tau', 0, 0, \tau'').$$

We can eliminate the integral in τ rewriting (see figure B1)

$$\int_0^\infty d\tau \int_{-\tau}^\infty d\tau' \int_{\tau+\tau'}^\infty d\tau'' = \int_0^\infty d\tau'' \int_{-\infty}^{\tau''} d\tau' \int_{\max(0,-\tau')}^{\tau''-\tau'} d\tau \tag{B.5}$$

and

$$\int_0^\infty d\tau \int_\tau^\infty d\tau'' \int_{\tau''-\tau}^\infty d\tau' = \int_0^\infty d\tau'' \int_0^\infty d\tau' \int_{\max(0,\tau''-\tau')}^{\tau''} d\tau. \tag{B.6}$$

Carrying on the integrals in τ by exploiting (B.4),

$$\hat{V} = -\frac{(d + 1)(d + 2)S^5 K^5 \hat{f}^2}{(d - 1)F^2} \int_0^\infty d\tau''\, h(\tau'') \left\{ \int_\infty^0 d\tau'\, G_1(\tau', \tau'') \right.$$

$$\left. + \int_0^{\tau''} d\tau'[G_2(\tau', \tau'') + G_4(\tau', \tau'')] + \int_{\tau''}^\infty d\tau'\, G_3(\tau', \tau'') \right\} \tau' h(-\tau'), \tag{B.7}$$
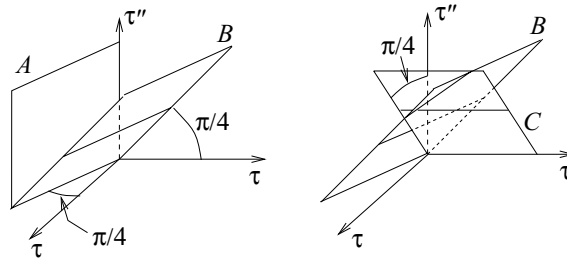
Figure B1. The domain for (B.5) is the wedge between planes *A* and *B* and the coordinate plane $\tau'\tau''$. The domain for (B.6) is the wedge between planes *B* and *C* and again the coordinate plane $\tau'\tau''$. The intersection of both planes *B* and *C* with the coordinate plane $\tau\tau''$ is the line $\tau'' = \tau$.

where the kernels G_μ ($\mu = 1, \ldots, 4$) get the following, simple expressions as the second condition in (20) allows us to Taylor expand the propagators ψ in τ' and τ'':

$$G_1(\tau', \tau'') \equiv \int_{-\tau'}^{\tau''-\tau'} d\tau\, \psi(\tau)\psi(\tau + \tau')\psi(\tau'' - \tau - \tau') \simeq -\frac{\tau'\tau''^3}{6} + \frac{\tau''^4}{12},$$

$$G_2(\tau', \tau'') \equiv \int_0^{\tau''-\tau'} d\tau\, \psi(\tau)\psi(\tau + \tau')\psi(\tau'' - \tau - \tau') \simeq -\frac{\tau'^4}{12} + \frac{\tau'^3\tau''}{6} - \frac{\tau'\tau''^3}{6} + \frac{\tau''^4}{12},$$

$$G_3(\tau', \tau'') \equiv \int_0^{\tau''} d\tau\, \psi(\tau)\psi(\tau'' - \tau)\psi(\tau - \tau'' + \tau') \simeq \frac{\tau'\tau''^3}{6} - \frac{\tau''^4}{12},$$

$$G_4(\tau', \tau'') \equiv \int_{\tau''-\tau'}^{\tau''} d\tau\, \psi(\tau)\psi(\tau'' - \tau)\psi(\tau - \tau'' + \tau') \simeq -\frac{\tau'^4}{12} + \frac{\tau'^3\tau''}{6}.$$

The desired result can then be obtained from (B.7) by specifying the exact form of the temporal correlation *h*; imposing (21), we finally get (22).

References

[1] Biferale L, Crisanti A, Vergassola M and Vulpiani A 1995 Eddy diffusivities in scalar transport *Phys. Fluids* **7** 2725–34
[2] Mazzino A 1997 Effective correlation times in turbulent scalar transport *Phys. Rev.* E **56** 5500–10
[3] Bender C M and Orszag S A 1978 *Advanced Mathematical Methods for Scientists and Engineers* (New York: McGraw-Hill)
[4] Castiglione P, Mazzino A, Muratore-Ginanneschi P and Vulpiani A 1999 On strong anomalous diffusion *Physica* D **134** 75–93
[5] Andersen K H, Castiglione P, Mazzino A and Vulpiani A 2000 Simple stochastic models showing strong anomalous diffusion *Eur. Phys. J.* B **18** 447–52
[6] Vergassola M and Avellaneda M 1997 Scalar transport in compressible flow *Physica* D **106** 148–66
[7] Pavliotis G A and Stuart A M 2005 Periodic homogenization for inertial particles *Physica* D **204** 161–87
[8] Maxey M R and Corrsin S 1986 Gravitational settling of aerosol particles in randomly oriented cellular flow fields *J. Atmos. Sci.* **43** 1112–34
[9] Maxey M R 1987 The motion of small spherical particles in a cellular flow field *Phys. Fluids* **30** 1915–28
[10] Maxey M R 1987 The gravitational settling of aerosol particles in homogeneous turbulence and random flow fields *J. Fluid Mech.* **174** 441–65
[11] Maxey M R 1990 On the advection of spherical and non-spherical particles in a non-uniform flow *Phil. Trans. R. Soc.* A **333** 289–307
[12] Aliseda A, Cartellier A, Hainaux F and Lasheras J C 2002 Effect of preferential concentration on the settling velocity of heavy particles in homogeneous isotropic turbulence *J. Fluid Mech.* **468** 77–105
[13] Friedman P D and Katz J 2002 Mean rise rate of droplets in isotropic turbulence *Phys. Fluids* **14** 3059–73

[14] Ruiz J, Macías D and Peters P 2004 Turbulence increases the average settling velocity of phytoplankton cells *Proc. Natl Acad. Sci.* **101** 17720–4

[15] Marchioli C, Fantoni M and Soldati A 2007 Influence of added mass on anomalous high rise velocity of light particles in cellular flow field: A note on the paper by Maxey (1987) *Phys. Fluids* **19** 098101:1–4

[16] Martins Afonso M 2008 On the terminal velocity of sedimenting particles in a flowing fluid *J. Phys. A: Math. Theor.* **41** 385501:1–15

[17] Grinshpun S, Redcoborody Y, Kravchuk S, Zadorozhnii V and Zhadanov V 2000 Particle drift in the field of an internal gravity wave *Int. J. Multiphase Flow* **26** 1305–24

[18] Eames I 2008 Settling of particles beneath water waves *J. Phys. Oceanogr.* **38** 2846–53

[19] Maxey M R and Riley J J 1983 Equation of motion for a small rigid sphere in a nonuniform flow *Phys. Fluids* **26** 883–9

[20] Hunt J, Perkins R and Fung J 1994 Review of the problem of modelling dispersed two-phase flows *Multiphase Sci. Technol.* **8** 595–643

[21] Michaelides E E 1997 Review: the transient equation of motion for particles, bubbles, and droplets *J. Fluids Eng.* **119** 233–47

[22] Magnaudet J and Eames I 2000 The motion of high-Reynolds-number bubbles in inhomogeneous flows *Annu. Rev. Fluid Mech.* **32** 659–708

[23] Wilkinson M and Mehlig B 2003 Path coalescence transition and its applications *Phys. Rev.* E **68** 040101:1–4

[24] Olla P and Vuolo M R 2007 Concentration fluctuations of large Stokes number particles in a one-dimensional random velocity field *Phys. Rev.* E **76** 066315:1–7

[25] Kraichnan R H 1968 Small-scale structure of a scalar field convected by turbulence *Phys. Fluids* **11** 945–53

[26] Kraichnan R H 1994 Anomalous scaling of a randomly advected passive scalar *Phys. Rev. Lett.* **72** 1016–9

[27] Douady S 1990 Experimental study of the Faraday instability *J. Fluid Mech.* **221** 383–409

[28] Gluckman B J, Arnold C B and Gollub J P 1995 Statistical studies of chaotic wave patterns *Phys. Rev.* E **51** 1128–47